Aryltriazene Photopolymers for UV-Laser Applications: Improved Synthesis and Photodecomposition Study

Matthias Nagel,* Roland Hany, Thomas Lippert, Martin Molberg, Frank A. Nüesch, Daniel Rentsch

An improved synthesis of photosensitive homopolymers containing aryltriazene chromophores covalently incorporated into the polymer backbone is reported. Such photopolymers proved to have promising properties for novel UV-laser applications. A homologous series of new aryltriazene polymers with increasingly branched side chains (R = Me, Et, iPr, *t*Bu) was synthesized and characterized. Homogeneous thin films with thicknesses from ≈15 to >150 nm were prepared by spin-coating. Photodecomposition was studied in solution and on thin films. Polymers with increasingly branched and bulky substituents showed decreasing photodissociation rates. NMR studies suggested an enhanced hindrance of the N(2)–N(3) bond rotation in the aryltriazene moiety with increasing steric demand of the substituents.

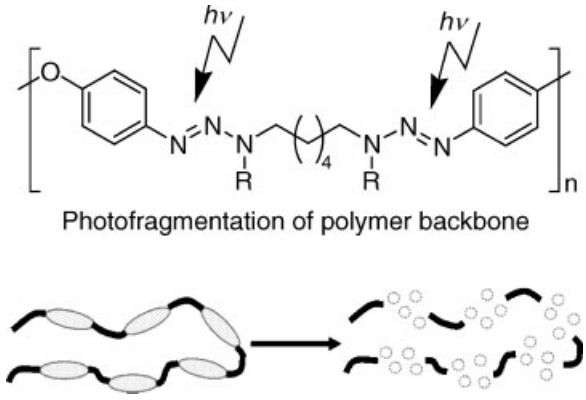

Introduction

Since the first reports about laser ablation of polymers in 1982, a wide variety of photopolymers tailored for laser-induced polymer processing, ranging from surface modification, ablative photodecomposition, to thin film deposition have been investigated.[1] Designed polymers, used as sacrificial absorbing layers for laser-induced forward transfer (LIFT) techniques, are increasingly finding applications in direct-writing operations for the controlled transfer and microdeposition of materials.[2] Various polymeric composite materials (usually a binder matrix doped with dispersed absorber dyes) have been applied as energy-absorbing dynamic release layer (DRL) systems, e.g., for high-resolution full-color printing,[3] transfer of single molecules[4] as well as biologic cellular systems,[5a–e] release of prefabricated parts in the assembly of microelectromechanical systems,[5f] or structured transfer of semiconducting polymers used in organic light-emitting diodes.[5g,5h] One of the common issues of these light-to-heat conversion layers based on IR-lasers is the intrinsically high thermal load on sensitive materials to be transferred.[6] In order to avoid overheating defects and heat-induced side-reactions,[6] we developed a modified concept of the LIFT process using a thin intermediate sacrificial photopolymer layer which is distinctly UV-sensitive

M. Nagel, R. Hany, F. A. Nüesch, D. Rentsch
Empa, Swiss Federal Laboratories for Materials Testing and Research, Laboratory for Functional Polymers, Überlandstrasse 129, CH-8600 Dübendorf, Switzerland
Fax: +41 44 823 40 12; E-mail: matthias.nagel@empa.ch
T. Lippert
Paul Scherrer Institute, CH-5232 Villigen PSI, Switzerland
M. Molberg
Technical University, D-64289 Darmstadt, Germany

DOI: 10.1002/macp.200600492

and decomposes photochemically more gentle into small and volatile fragments.[7]

Aryl-dialkyltriazene polymer films can be efficiently decomposed and ablated when irradiated with UV lasers.[1,8] Two Ar–N=N–NR_2 moieties as photolabile chromophores per repeating unit are covalently integrated into the polymer backbone (Scheme 2). Photolysis leads to a controlled photofragmentation with evolution of elemental nitrogen. Synthesis of the first aryltriazene homopolymer **TP-6a** was published in 1993,[9a] and, due to its favorable ablation characteristics,[1] it became an important reference compound within the last decade.[8,10] Related photocleavable polymers based on the arylazo parent system were synthesized, such as poly(alkylarylazosulfide)s[11] and poly(arylazophosphonate)s,[12] diazosulfonate polymer films,[13] triazene containing copolyesters,[14] and triazene-unit containing polyurethanes[15a,15b] as well as triazene polyacrylates.[15c] However, with regard to practical aspects like shelf-life, chemical compatibility, and their specific absorption range, triazene polymers are still the most attractive candidates for applications as the key part in photoinduced release layer systems.

For LIFT applications which require excellent film-forming properties,[2b,16] only thin polymer films with thickness of a few hundred nanometers at most are used. Until now, use of **TP-6a** as thin-film DRL was impeded due to its poor solubility and the formation of inhomogeneous solutions with crosslinked gel-type swollen lumps that are caused by undesirable side reactions. Here, we report the optimization of the synthetic protocol for **TP-6a** and a homologous series of new triazene homopolymers derived from it which all allow the fabrication of smooth thin films. We compare the photolytic decomposition of triazenes in solid state as well as in solution and discuss the influence of side-chain groups on the relative polymer stability subsequent to absorption.

Experimental Part

Synthesis of Triazene Homopolymers TP-6a–TP-6d

To 3.0 g of 4,4′-oxydianiline (**DAO**, 15 mmol) were added 30 mL of water and 7.5 mL of 37 wt.-% hydrochloric acid with stirring at room temperature. After complete dissolution of **DAO**, the solution was cooled to 0 to −5 °C and then 2.1 g sodium nitrite (30 mmol) dissolved in 20 mL of water was added dropwise within 10–15 min, keeping the temperature below 0 °C, and after complete addition, the yellow bisdiazonium salt solution was stirred for a further 15–20 min. The corresponding diamine component **DA-6** (15 mmol) was dissolved in 50 mL of ice-cold water containing 3.5 mL of conc. HCl. The two cold solutions were then added to a mixture of 150 g crushed ice and 100 mL of hexane. The biphasic mixture was mechanically stirred vigorously and 60 mL of a 2 M ice-cooled aqueous K_2HPO_4 solution (pH ≈ 8.5) was added from a dropping funnel. The color of the mixture changed slightly to dark yellow (pH 7–8). Then 60 mL of a cooled 2 M K_3PO_4 buffer solution (pH ≈ 12) was added dropwise. With rising pH values, the mixture became turbid and the precipitation of the polymer started from pH ≈ 8.5–9. The mixture became more viscous and after complete addition of the buffer solution, the pH of the reaction mixture was adjusted to 10–11 by the dropwise addition of 2 M KOH. The suspension was then stirred for 2–3 h while warming to room temperature. The light beige polymeric product was then filtered off and washed subsequently with hexane, *tert*-butyl methyl ether, isopropanol, methanol, and finally several times with water to remove inorganic salt residues. After drying overnight in a vacuum chamber, the raw polymer was dissolved in 120–150 mL of THF and the slightly viscous orange solution was then separated by centrifugation from a small fraction of insoluble viscous and dark residues. The supernatant clear polymer solution was then precipitated from 800 mL of methanol as sponge-like lumps, which were separated from the turbid solution by sieving. The product was washed with methanol and water and dried to a constant weight (yields > 85% related to the **DAO** starting material).

Synthesis of Disecondary Diamines DA-6a–DA-6d

Reactions were performed in a 1 L three-necked reaction vessel equipped with a 250 mL dropping funnel, thermometer, magnetic stirrer, and a chiller-cooled reflux condenser (−5–10 °C) with a gas reservoir on top to keep volatile amines in the reactor during the exothermic reaction. The monoamine (3 mol) dissolved in 100 mL THF was heated to 45–50 °C and a solution of 122 g 1,6-dibromohexane (0.5 mol) in 75 mL THF was added dropwise, such that a slight reflux is maintained. After addition of about half of the dibromoalkane, the mixture became more and more turbid and crystalline mass started to precipitate and after complete addition of 1,6-dibromohexane, the mixture was stirred for 3 h at a slight reflux. A concentrated aqueous solution of 68 g of KOH (1.2 mol) dissolved in ≈40 g crushed ice was added and the resulting mixture stirred over night at room temperature. The excess of monoamine and THF were distilled off at atmospheric pressure, the remaining waxy mass was suspended in 300 mL of toluene and water was then removed by azeotropic distillation. The crystalline mass of KBr could easily be separated from the organic phase by filtration. The solid phase was washed twice with toluene and the solvent distilled off from the collected organic filtrate fractions under reduced pressure. The remaining oil was purified by fractional distillation which gave the diamines as highly hygroscopic colorless liquids.

Characterization

NMR experiments were performed on a Bruker Avance-400 spectrometer using a 5 mm broadband inverse probe with z-gradient. Measurements were carried out at 297 K with ≈30 mg of sample dissolved in 0.7 mL of solvent. Chemical shifts are given in ppm relative to the remaining signals of chloroform at 7.26 ppm

Macromol. Chem. Phys. **2007**, *208*, 277–286

Macromolecular Journals

DOI: 10.1002/macp.200600492

(^{1}H) and 77.7 ppm (^{13}C). For ^{1}H, ^{13}C 2D correlation experiments, Bruker standard pulse programs and parameters were used.

TP-6a: ^{1}H NMR: $\delta = 1.38$ [m, –N–$(CH_2)_2$–CH_2–], 1.67 (m, –N–CH_2–CH_2–), 3.18 (s, –N–CH_3), 3.71 (t, $J = 7.2$ Hz, –N–CH_2–CH_2–); 6.96, 7.37 (Ar–H). ^{13}C NMR: $\delta = 27.1$ [$\Delta\nu_{1/2} \approx 3.5$ Hz, –N–$(CH_2)_2$–CH_2–], 28.8 ($\Delta\nu_{1/2} \approx 17$ Hz, –N–CH_2–CH_2–), 35.9 ($\Delta\nu_{1/2} \approx 65$ Hz, –N–CH_3), 55.3 ($\Delta\nu_{1/2} \approx 95$ Hz, –N–CH_2–CH_2–); 119.8, 122.2, 147.5, 155.9 (Ar–C). **TP-6b**: ^{1}H NMR: $\delta = 1.23$ (t, $J = 7.1$ Hz, –N–CH_2–CH_3), 1.40 [m, –N–$(CH_2)_2$–CH_2–], 1.69 (m, –N–CH_2–CH_2–), 3.67 (≈t, $J = 7.2$ Hz, –N–CH_2–CH_2–), 3.72 (q, $J = 7.2$ Hz, –N–CH_2–CH_3); 6.96, 7.36 (Ar-H). ^{13}C NMR: $\delta = 13.6$ (–N–CH_2–CH_3), 27.4 [–N–$(CH_2)_2$–CH_2–], 28.4 (–N–CH_2–CH_2–), 45.5 (–N–CH_2–CH_3), 51.0 (–N–CH_2–CH_2–); 119.9, 122.1, 147.6, 155.8 (Ar-C). **TP-6c**: ^{1}H NMR: δ 1.32 [d, $J = 6.6$ Hz, –N–CH–$(CH_3)_2$], 1.39 [m, –N–$(CH_2)_2$–CH_2–], 1.67 (m –N–CH_2–CH_2–), 3.58 (≈t, $J = 7.4$ Hz, –N–CH_2–CH_2–), 4.17 [broad, –N–CH–$(CH_3)_2$]; 6.96, 7.36 (Ar-H). ^{13}C NMR: $\delta = 22.2$ [–N–CH–$(CH_3)_2$], 27.7 [–N–$(CH_2)_2$–CH_2–], 28.0 (–N–CH_2–CH_2–), 46.6 (–N–CH_2–CH_2–); 119.7, 122.1, 147.9, 155.7 (Ar-C); [–N–CH–$(CH_3)_2$ not detected]. **TP-6d**: ^{1}H NMR: $\delta = 1.39$ [m, –N–$(CH_2)_2$–CH_2–], 1.43 [s, –N–C$(CH_3)_3$], 1.62 (m, –N–CH_2–CH_2–), 3.62 (m, –N–CH_2–CH_2–). ^{13}C NMR: $\delta = 27.9$ [–N–$(CH_2)_2$–CH_2–], 28.2 (–N–CH_2–CH_2–), 29.8 [–N–C$(CH_3)_3$], 44.4 (–N–CH_2–CH_2–); 119.7, 122.2, 148.2, 155.6 (Ar-C); [–N–C$(CH_3)_3$ not detected].

DA-6a: ^{1}H NMR: $\delta = 1.12$ (–NH), 1.27 [m, –N–$(CH_2)_2$–CH_2–], 1.41 (m, –N–CH_2–CH_2–), 2.35 (s, –N–CH_3), 2.49 (t, $J = 7.1$ Hz, –N–CH_2–CH_2–). ^{13}C NMR: $\delta = 27.9$ [–N–$(CH_2)_2$–CH_2–], 30.5 (–N–CH_2–CH_2–), 37.1 (–N–CH_3), 52.7 (–N–CH_2–CH_2–). **DA-6b**: ^{1}H NMR: $\delta = 0.7$ (–NH), 0.96 (t, $J = 7.2$ Hz, –N–CH_2–CH_3), 1.20 [m, –N–$(CH_2)_2$–CH_2–], 1.35 (m, –N–CH_2–CH_2–), 2.46 (t, $J = 7.2$ Hz, –N–CH_2–CH_2–), 2.50 (q, $J = 7.2$ Hz, –N–CH_2–CH_3). ^{13}C NMR: $\delta = 15.8$ (–N–CH_2–CH_3), 27.8 [–N–$(CH_2)_2$–CH_2–], 30.6 (–N–CH_2–CH_2–), 44.6 (–N–CH_2–CH_3), 50.3 (–N–CH_2–CH_2). **DA-6c**: ^{1}H NMR: $\delta = 0.9$ (–NH), 1.00 [d, $J = 6.3$ Hz, –N–CH–$(CH_3)_2$], 1.30 [m, –N–$(CH_2)_2$–CH_2–], 1.44 (m, –N–CH_2–CH_2–), 2.54 (t, $J = 7.2$ Hz, –N–CH_2–CH_2–), 2.74 [septett, $J = 6.3$ Hz, –N–CH–$(CH_3)_2$]. ^{13}C NMR: $\delta = 23.7$ [–N–CH–$(CH_3)_2$], 28.1 [–N–$(CH_2)_2$–CH_2–], 31.1 (–N–CH_2–CH_2–), 48.2 (–N–CH_2–CH_2–), 49.4 [–N–CH–$(CH_3)_2$]. **DA-6d**: ^{1}H NMR: $\delta = 0.56$ (–NH), 0.96 [s, –N–C$(CH_3)_3$], 1.22 [m, –N–$(CH_2)_2$–CH_2–], 1.32 (m, –N–CH_2–CH_2–), 2.40 (t, $J = 7.2$ Hz, –N–CH_2–CH_2–). ^{13}C NMR: $\delta = 28.1$ [–N–$(CH_2)_2$–CH_2–], 29.7 [–N–C$(CH_3)_3$], 31.8 (–N–CH_2–CH_2–), 43.1 (–N–CH_2–CH_2–), 50.7 [–N–C$(CH_3)_3$].

CHN contents were determined on a varioEL (Foss-Heraeus). **TP-6a** $(C_{20}H_{26}N_6O)_n$ $(366.46)_n$: Calcd. C 65.55, H 7.15, N 22.93; Found C 65.48, H 7.18, N 23.05. **TP-6b** $(C_{22}H_{30}N_6O)_n$ (394.51): Calcd. C 66.98, H 7.66, N 21.30; Found C 66.78, H 7.63, N, 21.3. **TP-6c** $(C_{24}H_{34}N_6O)_n$ $(422.57)_n$: Calcd. C 68.22, H 8.11, N 19.89; Found C 68.04, H 8.09, N 20.06. **TP-6d** $(C_{26}H_{38}N_6O)_n$ $(450.63)_n$ Calcd. C 69.30, H 8.50, N 18.65; Found C 68.63, H 8.46, N 18.75.

Gel-permeation chromatography experiments were performed on a Agilent 1100 series system with PSS-SDV (5 μm, 100 Å, and 1 000 Å, 8.0 × 300 mm) columns and UV-RI detectors. THF was used as eluent applying polystyrene standards from Polymer Standards Services (PSS-ReadyCal Kit, $\overline{M}_p = 376$–2 570 000 Da) for calibration. Polymer solutions were filtered by a 0.45 μm syringe filter (PTFE, Titan-2) before injection.

Thermogravimetric measurements were performed on a Perkin–Elmer Thermobalance TGA 7 with a heating rate of 20 K · min^{-1} from 30 to 900 °C in a He atmosphere, and differential scanning calorimetry measured on a Perkin–Elmer power-compensation difference calorimeter model DSC 7: capped 50 μL Al pan, calibration with indium, heating rate 20 K · min^{-1}, N_2 atmosphere, 2 measurements per sample, values taken from the second cycle each.

Thin Films and Photolysis Studies

FFilms were prepared by spin-coating polymer solutions (in a 1:1 w/w mixture of cyclohexanone and chlorobenzene) onto glass or quartz substrates (Suprasil 2) in a laminar flow hood. Substrates were cleaned before coating by subsequent washing with acetone, ethanol, and Hellmanex® solution (each under sonication), and finally by rinsing with pure water (Millipore quality). 0.2–0.3 mL of polymer solutions were applied on the substrate with a syringe equipped with a filter (0.45 μm or 0.2 μm, depending on the viscosity). Solutions with 2–3 wt.-% in polymer content gave films with thicknesses of ≈100 nm (1 500–2 000 rpm, ramp 500 rpm · s^{-1}). Films were dried for 2 h at 40–50 °C on a heating plate and then stored over night in a vacuum chamber at reduced pressure to remove solvent residues.

Film thickness and surface roughness measurements were performed on an Ambios Technology XP-1 profilometer from Atomic Force, with a stylus force of 0.05 mg. Absorbance spectra were measured with a Cary50 UV-Vis spectrophotometer. Films with a thickness of ≈100 nm showed absorbance values of ≈1.0 at the maximum of the triazene band at ≈330 nm. A linear correlation between the film thickness determined by profilometry and the corresponding absorbance was found for each of the polymers.

Irradiation experiments were performed at room temperature with a high-pressure mercury vapor lamp (Hanau, TQ 25 double wall, water-cooled, electrical power 25 W) placed at a distance of 20 cm from the probe, equipped with a light channel (18 cm), a mechanical shutter, and a long-pass glass filter (Schott WG-280, 2 mm, UV cut-off <260 nm) mounted at the end of the channel. Films coated on quartz substrates were mounted on a support and irradiated with the film side oriented towards the lamp. Absorption spectra were recorded after known exposure-time intervals. In the same way, photodegradation experiments of dilute polymer solutions (≈10^{-6} mol · L^{-1} repeating units) in THF (spectroscopic grade, degassed with argon) were performed in stopped quartz cuvettes with stirring.

Results and Discussion

Reported Polymer Synthesis

According to the literature protocol[9a,9b] summarized in Scheme 1, the synthesis of **TP-6a** starts with the transformation of bisaniline precursor, **DAO**, into its bisdiazonium salt derivative, **BDS**, by a diazotation reaction.[17] The acidic solution of the freshly prepared **BDS** is then treated with an excess of sodium carbonate dissolved in water, raising the pH to strongly alkaline values. Subsequently, a solution of diamino compound **DA-6a** dissolved in hexane is added, and the interfacial polycondensation reaction starts immediately. The polymer is insoluble in both phases and precipitates as beige flakes which are filtered

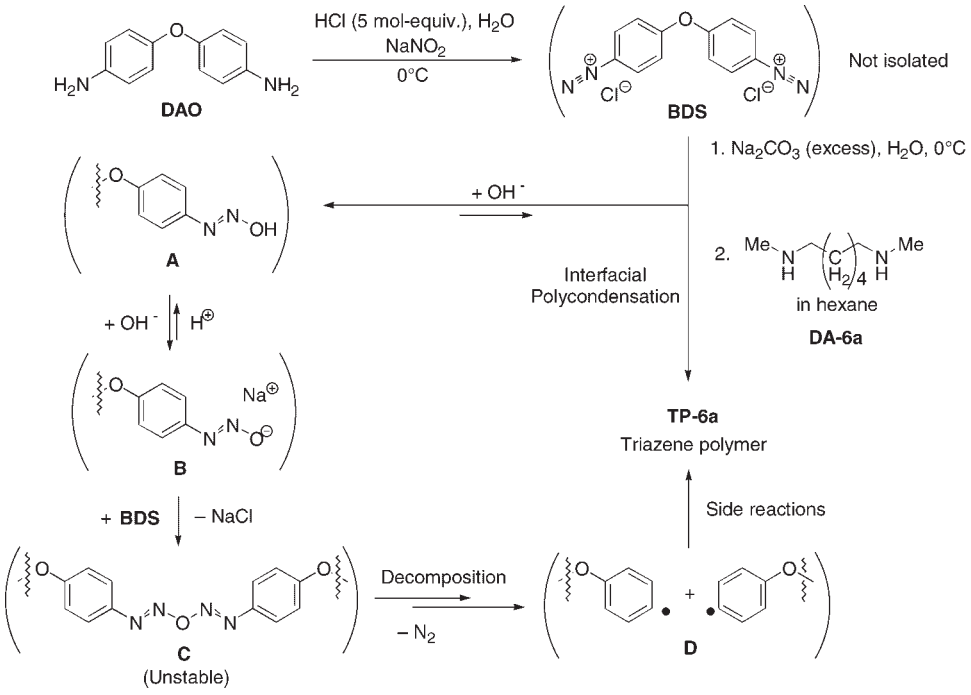

Scheme 1. Reported synthetic route to triazene homopolymer **TP-6a**[9a], including origin of reactive intermediates and side reactions.

off. For purification, a solution of the polymeric reaction products in THF is precipitated in methanol, and the reported yields are 63% of **TP-6a** related to **DAO**.[9b] Following the protocol repeatedly, the colors of our polymeric products ranged from light-beige to brown. The darker products had significantly lower solubility in THF and the solutions were more viscous or even gel-like (Figure 1). Therefore, the purification step was impeded by the low solubility of some polymer batches and yields were low. Attempts to spin-coat such viscous polymer solutions into homogeneous thin films failed.

We attribute these findings to side reactions that induce crosslinking reactions in parallel to polymerization (Scheme 1): One significant drawback of the reported synthesis is the inhomogeneous reaction conditions during the addition of **DA-6a**. It can only be added slowly, since the elimination of HCl formed during the condensation step leads to the formation of CO_2 bubbles. The precipitating polymer suspension, therefore, forms a foaming mixture that is difficult to homogenize, and insufficient neutralization conditions can induce a protolytic back- cleavage of the formed triazene polymer.[8,9c,18]

In addition, alkaline solutions of **BDS** are unstable and we noticed a progressive darkening after addition of sodium carbonate. When **DA-6a** was added to "aged" solutions of **BDS**, mainly dark-colored and only partly soluble products were obtained. In alkaline solutions, aryldiazonium compounds decompose with the evolution of molecular nitrogen, forming aryl radicals that recombine to biaryl species (Gomberg–Bachmann reaction):[19a–d] In the presence of hydroxide ions, **BDS** is transformed in part into diazohydroxide intermediates (Scheme 1, species **A**) that, with increasing pH values, are deprotonated and transformed into diazotates (**B**). **B** reacts with a further diazonium moiety into diazoanhydride compounds **C** that decompose quickly with evolution of N_2 into arene radicals **D**. The interfering side reactions (**A** → **D**) start immediately after reaching alkaline pH values, and thus before **DA-6** itself is added. Therefore, depending on the speed of addition of the coupling compound, the competing reactions lead to arene radical species **D** at the same time. These attack either aryl moieties of the starting

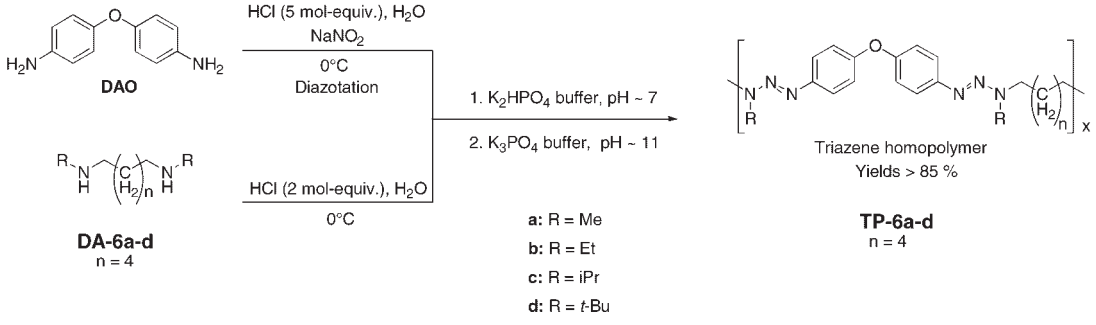

Scheme 2. Improved synthetic route via an interfacial polycondensation reaction to triazene homopolymers **TP-6a**–**TP-6d**.

Macromol. Chem. Phys. **2007**, *208*, 277–286

DOI: 10.1002/macp.200600492

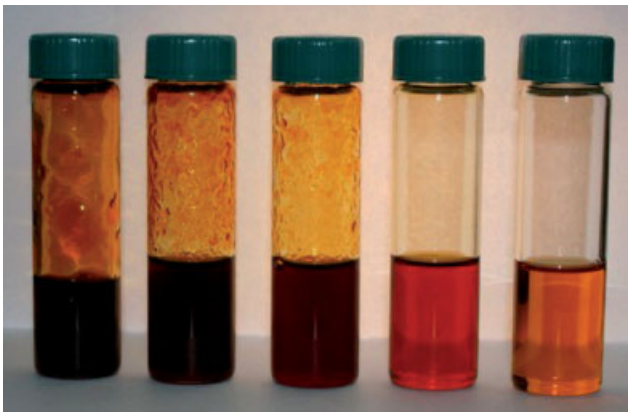

Figure 1. Visualization of the improvement process: Solutions of different batches of **TP-6a** (each 5 wt.-% in cyclohexanone/chlorobenzene, 1:1) after turning the samples once upside down. From left to right: three flasks with polymer synthesized according to the reported synthesis show dark color, high viscosity, and inhomogeneous gel-type swollen lumps sticking at the glass walls. The flask on the right finally contains **TP-6a** prepared according to the optimized synthetic procedure which exhibits excellent film-forming properties.

materials or of already formed triazene-polymer chains, causing crosslinking and chain termination.

Improvement of the Synthetic Protocol

In order to circumvent these problems, the reaction conditions for the polycondensation were adapted (Scheme 2). First, the carbonate solution was replaced by a non-effervescent neutralizing agent that allows a reproducible pH control of the reaction mixture. In order to avoid local high alkali concentrations, we chose the phosphate buffer system that allows to adjust a controlled pH gradient by adding solutions of K_2HPO_4 (pH ≈ 8.5) and K_3PO_4 (pH ≈ 12, each 2 M in water). Furthermore, **DA-6a** was converted into its water-soluble bishydrochloride derivative. This component can then be added in aqueous solution as a protected reactant directly to the acidic solution of the bisdiazonium salt without any interaction. With both reaction components in the reaction mixture, the polycondensation reaction can be triggered by raising the pH of the reaction mixture up to ≈8, where the diamino compound is liberated from its corresponding "protected" ammonium precursor form. The in situ liberated bisamine **DA** gets dissolved in the organic phase (hexane) of the biphasic reaction mixture and the interfacial polycondensation starts. Subsequently, the pH is increased by addition of K_3PO_4 and the precipitation of the polymer typically started at pH ≈9, where the unwanted formation of diazotates in the equilibrium is negligible (Scheme 1, **B**). The polymeric products were dissolved in THF and precipitated from methanol (yields relative to **DAO** > 85–90%).

Physical Properties

All GPC curves showed a similar profile with average polydispersity values D in the range of 4.5–5.0 (Table 1); these are typical values for an interfacial polycondensation. Number- and mass-average molar masses ranged from 25 000 to 45 000 $g \cdot mol^{-1}$ for $\overline{M}_n$, and 140 000 to 180 000 $g \cdot mol^{-1}$ for $\overline{M}_w$. For **TP-6a**, these values are different from those of former batches synthesized according to the published protocol,[9a] where we obtained $\overline{M}_n$ and $\overline{M}_w$ of ≈15 000 and ≈70 000 $g \cdot mol^{-1}$, in accordance with the published values.[9a,9b] The higher molar masses of the new **TP-6** series suggest that the modified reaction conditions avoid uncontrolled chain terminations. All polymers started to decompose at a temperature of ≈230 °C.

NMR Studies

The ^1H NMR spectra of **TP-6a**–**TP-6d** in Figure 2 demonstrate the purity of the triazene polymers. The protons of

Table 1. Average yields and physical properties of triazene homopolymers TP-6.

TP	Yield	$\overline{M}_n$ [a,b]	$\overline{M}_w$ [a,b]	M_{max} [a,b]	D [a]	T_g [c]	T_D [d]
		$g \cdot mol^{-1}$	$g \cdot mol^{-1}$	$g \cdot mol^{-1}$		°C	°C
TP-6a-R[e]	63%	15 000	71 000	30 000	4.7	63	227
TP-6a	85–95%[a]	28 000	140 000	105 000	5.0	47	225–230
TP-6b	90–95%[a]	35 300	162 000	115 000	4.5	29	225–230
TP-6c	80–90%[a]	43 000	182 000	138 500	4.4	38	225–230
TP-6d	85–90%[a]	30 000	143 000	120 300	4.8	87	225–235

[a] Average values of at least three batches; [b] $\overline{M}_n$, $\overline{M}_w$: number- and mass-average molar masses; M_{max} molar mass at the maximum of the GPC curve; [c] Glass transition temperature; [d] Beginning of weight loss; [e] Reference polymer corresponding to TP-6a; values taken from ref.[9a,9b].

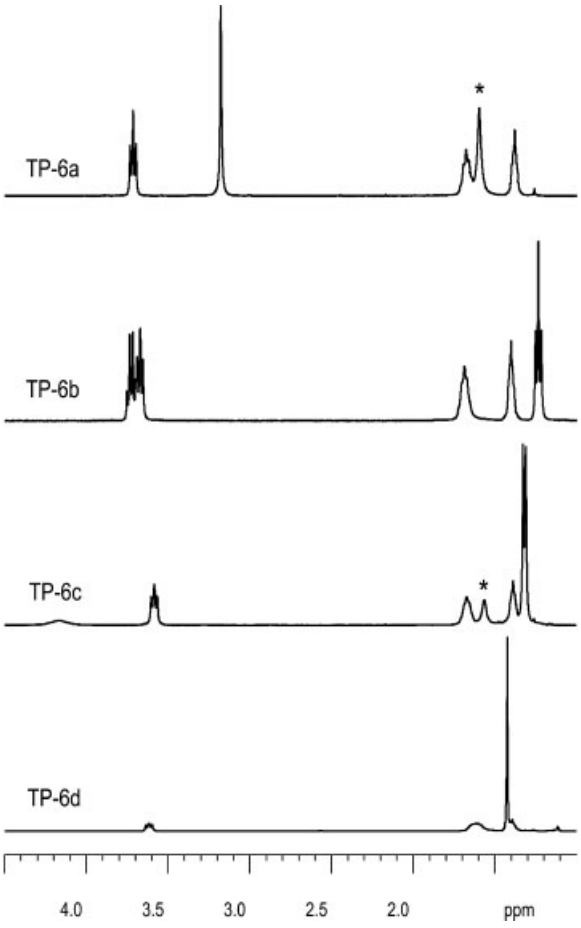

Figure 2. Aliphatic parts of ^{1}H NMR spectra of triazene polymers **TP-6a–TP-6d**. The residual water signal in the solvent $CDCl_3$ is marked with * for **TP-6a** and **TP-6c**.

the methylene groups attached to N(3) of the triazene moieties show broadened signals. As for most 1-aryl-3,3-dialkyltriazenes, the N(2)–N(3) bond rotation is restricted.[20d] This effect is ascribed to partial π-bond formation between N(2) and N(3).[14d,20a,20b] Therefore, NMR resonances for $-N(1)=N(2)-N(3)<$ alkyl substituents are broadened, and the rotation barrier has been quantitatively evaluated with variable-temperature NMR experiments for various 1-aryl-3,3-dialkyltriazene derivatives (coalescence temperatures $T_C \approx 230 - > 310$ K).[20c,20d] The hindered rotation of the dialkylamino group fixes the N(3)-alkyl substituents in a position either *cis* or *trans* to the azo group which itself tends to adopt the sterically less hindered *trans* configuration.[14d,20b,20c] The rotation barrier is strongly dependent on electronic effects of the substituent groups. Strong electron-withdrawing groups on the aromatic ring favour the 1,3-dipolar resonance structure and the *cis* and *trans* rotamers are distinct even at room temperature.[20b–d] Increasing line widths of the $-N(3)-\underline{C}H_2-CH_2-$ resonances from $\Delta\nu_{1/2} \approx 1.7$ Hz for **TP-6a** and **TP-6b**, to 2.2 Hz for **TP-6c** and 2.6 Hz for **TP-6d** were observed. This suggests that increasing rotational hindrance also occurs with increasing steric demand and mass of the N(3)-alkyl substituents.[20d,21] The hindered rotation affected the ^{13}C NMR spectra much stronger. For example, line widths of $\Delta\nu_{1/2} \approx 100$ Hz for $-N(3)-\underline{C}H_2-$ and ≈70 Hz for $-N(3)-\underline{C}H_3$ of **TP-6a** were determined from the 1D ^{13}C NMR spectrum. For other polymers, the alkyl carbon resonances were significantly broader, and ^{13}C chemical shifts were obtained from 2D correlated ^{1}H, ^{13}C-HSQC spectra.

Parts of ^{1}H NMR spectra of **TP-6c** at different temperatures are shown in Figure 3. At 297 K, the two nonequivalent *i*-C_3H_7 methine protons are close to coalescence with a broad signal at 3.80 ppm ($\Delta\nu_{1/2} \approx 90$ Hz). At higher temperatures the signal narrows, whereas distinct signals for the two isomers appear at 3.72 ppm and 5.17 ppm at 280 K. Due to steric requirements, we suggest that the *iso*-propyl group of the favoured isomer (≈90%) is in *trans* position relative to the azo group (Figure 3). The large chemical shift difference ($\Delta\nu \approx 590$ Hz) for the two methine protons results in a coalescence temperature around 290 K.

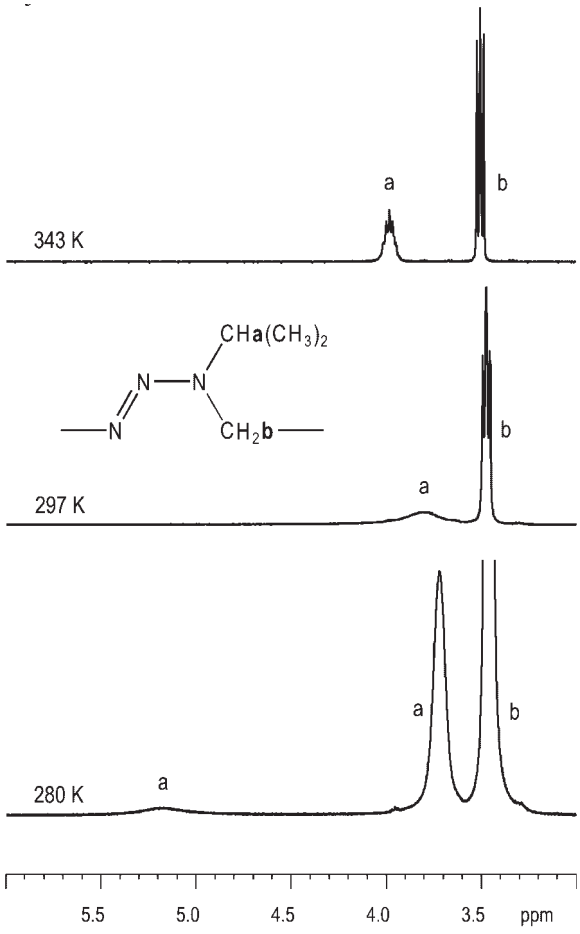

Figure 3. Parts of ^{1}H NMR spectra of **TP-6c** in d_8-toluene at different temperatures.

Macromol. Chem. Phys. **2007**, *208*, 277–286

DOI: 10.1002/macp.200600492

The other alkyl resonances broaden with decreasing temperature, but coalescence was not reached. The line widths of the aryl proton signals were not temperature dependent.

Photodegradation Studies

UV-Vis spectra of all polymers are similar and show three strong main absorption bands at ≈200, 290, and 330 nm,

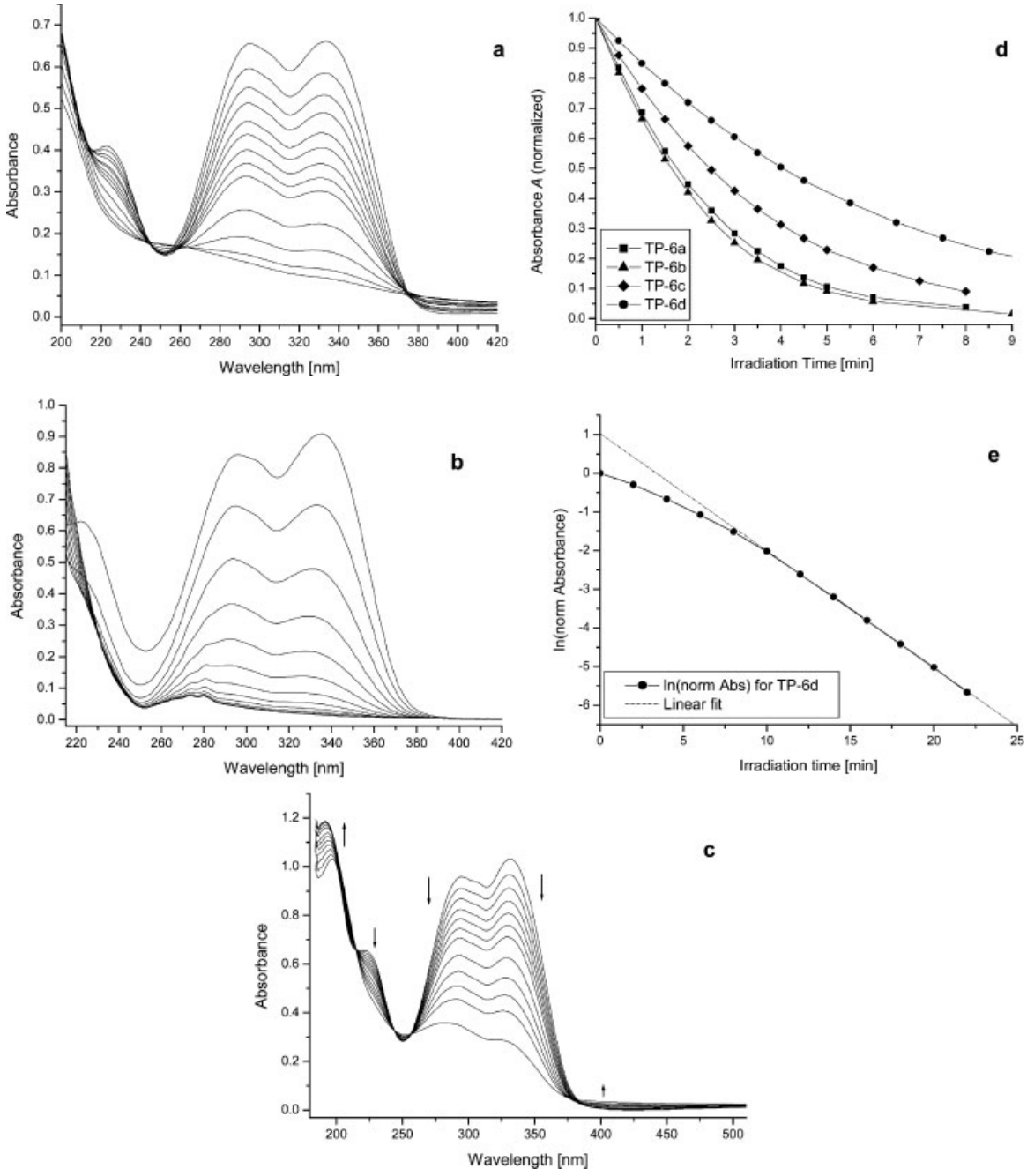

Figure 4. Initial UV absorption curve and photodecomposition of triazene polymers: (**a**) ≈70 nm thick film of **TP-6d** on a quartz substrate, irradiated with a mercury lamp. UV spectra were recorded after successive irradiation intervals of 2, 4,. . .16, 22, 30, 40, and 50 min; (**b**) **TP-6d** in THF solution for the same irradiation conditions as for (a). UV spectra were recorded after 2, 4, . . . 22 min; (**c**) ≈100 nm thick film of **TP-6a** on a quartz substrate, irradiated with a XeCl* excimer lamp at 308 nm. Spectra were recorded after 1, 2, 3, . . . 6, 8, 10, 12, 14, and 18 min; (**d**) Decrease of $A(t)$ for the photolytic decomposition of **TP-6a**-**TP-6d** in THF solution (recorded each at λ_{max}, A_o normalized to 1); (**e**) Kinetic plot ln [$A(t)$] versus irradiation time t for **TP-6d** in THF solution. Rate constants k were derived from the linear parts for $A < \approx 0.3$ (i.e. ln $A < \approx -1$).

and a weaker band at 220 nm appears as a pronounced shoulder (Figure 4). The absorption maximum at 330 nm is attributed to the characteristic aryltriazene band of a π–π^* transition in the azoamine chromophore.[1] Values for the maximum molar decadic absorption coefficient ε vary between 31 400 and 33 400 $L \cdot mol^{-1}cm^{-1}$ related to the molar mass of the repeating units (Table 2). Excitation of the triazene band leads to cleavage of the photolabile chromophore with release of elementary nitrogen.[1,9c,22] The absorption measurements show the progressive decomposition of the photolabile triazene chromophore when the polymers were exposed to irradiation: both bands at 290 and 330 nm, as well as the shoulder at 220 nm get weaker, whereas the aromatic absorption bands at 200 nm increase upon irradiation (Figure 4).

Photolysis of Thin Films

Polymer films with thickness between ≈15 and ≈100 nm were investigated. Average roughness of the film surfaces were typically below 10 nm, which corresponds to the roughness of the substrate surfaces. A typical example for the change in the UV absorption curve during photodecomposition is shown in Figure 4(a) for a 70 nm thick film of **TP-6d**. For the kinetic analysis, the decrease of absorbance A at the maximum wavelength λ_{max} was followed as a function of irradiation time t. From the corresponding kinetic equation $A(t) = A_0\ e^{-kt}$, rate constants k for each polymer were derived according to $kt = \ln [A_0 - A_\infty] - \ln [A(t) - A_\infty]$, where A_0 is the initial absorbance before photolysis, and A_∞, the remaining absorption after complete photodecomposition. Linear fits in such plots indicating first-order kinetics were found for absorbance values below ≈0.3 in the later part of the irradiation experiments, or for films thinner than ≈30 nm [cf. Figure 4(e)]. For thicker films, the initial stages of the photolysis proceeded according to transient pseudo zero-order kinetics due to the high optical density of the films. The specific half-life time $\tau_{1/2} = \ln 2/k_{rel}$ of reference polymer **TP-6a**, derived from the linear part in the plot, was 2.96 min, and the corresponding $\tau_{1/2}$ values increased steadily to 10.56 min for **TP-6d** (Table 2). Absolute rate constants are dependent on the experimental setup and only partly meaningful. Therefore, k_{rel} ratios relative to $k_{\mathbf{TP\text{-}6a}} = 1.0$ as the standard reference are summarized in Table 2 as well. The photochemical reactivity within the polymer series is decreasing with the increasing steric demand of side-chain substituents R.

Photodecomposition in Solution

For comparison, photolysis was performed in THF solutions. The experimental setup (lamp, distance of target from light source) of the experiments described above were maintained. Therefore, the kinetic results of the two sets of experiments should remain comparable. Figure 4(b) depicts the photodecomposition of polymer **TP-6d** with time intervals of 2 min each. With a similar initial absorbance A_0, the photolysis is significantly faster in solution compared to films (Table 2). The absorption band of the triazene chromophore flattens first and then disappears completely, indicating a high degree of polymer photodecomposition. The aromatic band at ≈200 nm increases significantly but cannot be measured reliably, since the strong absorption of the solvent THF interferes in this spectral domain.

As for the films, kinetic analysis revealed linear fits for absorbances less than ≈0.3. Literature results[9b] showed that in the related aryltriazene polymers, an increasing degree of substitution of linear side chains R (with R = Me, Et, Pr) resulted in enhanced photodecomposition ($k_{rel} > 1$).

Table 2. UV Spectral Characteristics and Photolysis Kinetic Data.

TP	λ_{max} [a]	$\varepsilon(\lambda_{max})$ [b] (solution)	k_{rel} [c,d]; $\tau_{1/2}$ (solution)	k_{rel} [c,d]; $\tau_{1/2}$ (thin film)	$\tau_{1/2film}/\tau_{1/2soln}$ [c,d]	k_{rel} [c)e] (thin film)
	nm	$L \cdot mol^{-1} \cdot cm^{-1}$	(Hg lamp); min	(Hg lamp); min	Hg lamp	XeCl lamp
TP-6a-R [f]	332	30 600	–	–	–	–
TP-6a	332	32 500	≡1.0; (1.45)	≡1.0; (2.96)	≈2.0	≡1.0
TP-6b	335	33 200	1.12; (1.30)	0.79; (3.73)	≈2.9	0.68
TP-6c	336	33 400	0.64; (2.29)	0.44; (6.75)	≈2.9	0.52
TP-6d	333	31 400	0.40; (3.5)	0.28; (10.56)	≈3.0	0.42

[a] Wavelength at the absorption maximum in THF; [b] Related to the molar mass of repeating units; [c] Relative ratio of absolute values $k_{TP\text{-}6}/k_{TP\text{-}6a}$ for identical irradiation conditions; [d] Irradiation with a mercury lamp; [e] Monochromatic irradiation with a XeCl* excimer lamp at 308 nm; [f] Reference polymer corresponding to TP-6a; values taken from ref.[9a,9b].

Macromol. Chem. Phys. **2007**, *208*, 277–286

Macromolecular Journals

DOI: 10.1002/macp.200600492

This behavior was also observed for the polymers **TP-6a** and **TP-6b** (Table 2). According to the given explanation that the increasing steric demand of side chain substituents at N(3) of the triazene chromophore decreases the ability of recombination of the formed radicals, we expected that photodecomposition of **TP-6c** and **TP-6d** also exhibited values $k_{rel} > 1$. However, for the branched *iso*-propyl and *tert*-butyl substituted polymers, the decomposition rates significantly slowed down. The recombination is influenced by the stability and lifetime of radical intermediates. Increasing inductive effects of substituents R will increase the stability of these radicals, allowing for more recombination before N_2 is released. This then explains that rates for photodecomposition of polymers with branched side chains slowed down as observed.

A further hypothesis to explain the decreasing photodecomposition rates from **TP-6a** to **TP-6d** is based on photolysis and thermolysis studies of structurally related poly(alkylaryldiazosulfide)s[11a] and diarylpentazadiene compounds.[23] The authors revealed an enhanced photolability of the −N=N− *Z*-configuration and suggested a photoinduced $E \leftrightarrow Z$ rearrangement as an intermediate reaction step. If a *Z*-configuration is also favoring photodissociation for triazenes, we assume that increasing steric demand and mass of the N(3)-alkyl substituents hinder the *E*/*Z* isomerization step. This would also be in qualitative agreement with our NMR studies where we observed an increasing rotational hindrance about the N(2)–N(3) bond from **TP-6a** to **TP-6d**.

A significant difference between decomposition in solution and in films consists in the remaining basic absorbance of the characteristic triazene twin bands [Figures 4(a) and 4(b)]. The residual absorbance of the triazene bands is minimal in solution [Figure 4(b)], since most of the formed radicals are immediately quenched by disproportionation reactions with the surplus of the surrounding solvent THF. In contrast, photodegraded polymer films show a significant remaining absorption even after long irradiation times [Figure 4(a)]. We attribute this to the formation of conjugated polyarene species. After cleavage and release of N_2, the remaining closely packed aryl radical species can recombine within the film, forming crosslinked conjugated arene networks that absorb at longer wavelength. We found a reduced solubility of irradiated film areas when the substrates were cleaned by rinsing with THF. Additionally, microscopic analysis confirmed a slightly shady and turbid clouding of irradiated domains, indicating a change in homogeneity and refractive index of the former clear films.

Excimer-Lamp Irradiation Experiments

With regard to practical applications, polymer films were also investigated with quasi-monochromatic irradiation of a $XeCl^*$ excimer lamp at 308 nm.[24] A plot of UV curves is shown in Figure 4(c) for a 100 nm thick film of **TP-6a**. With the narrow-band excitation, all curves intersect properly at four isosbestic points, indicating a uniform mechanism of the photodecomposition process. **TP-6b**–**TP-6d** showed similar curves with sharp isosbestic points. Only the main absorption bands of the triazene chromophores are excited at 308 nm, whereas the polychromatic UV light of the mercury arc lamp excites several electronic transitions simultaneously below 400 nm. Therefore, more complex photodecomposition processes are induced, which have an influence on the pathway of photofragmentation reactions.[1] In agreement with the mercury lamp photolysis experiments, decreasing rate constants were found for **TP-6a** to **TP-6d** with increasing steric demand of the alkyl substituents attached to the triazene moiety (Table 2).

Conclusion

The modified synthesis provides access to triazenes as pure and soluble high-molecular mass compounds in high yields. Photodecomposition of films decreases with the increasing steric demand of the side-chain substituents, and a clean first order decomposition kinetic was found for monochromatic irradiation at 308 nm for all polymer films with an absorbance below 0.3. The promising potential of these materials in LIFT applications was demonstrated with highly sensitive materials recently: assisted by a ≈100 nm thick sacrificial DRL of polymer **TP-6a**, living mammalian neuroblast cells were transferred and gently deposited on a receiver substrate.[7] In the same way, multi-spectral nanocrystal quantum dots (NCQD) were successfully transferred by the **TP-6a**-film-assisted LIFT setup into laterally patterned arrays.[25]

Acknowledgements: We thank *T. Geiger* and *M. Schmid* for GPC measurements and *B. Fischer* and *C. Löwe* for TGA and DSC analyses. The assistance of *R. Fardel* and *L. Urech (PSI)* at experiments with the excimer lamp is gratefully acknowledged, as well as *H. Benmansour* for helpful discussions. Financial support for this project was granted by *Empa*.

Received: September 29, 2006; Accepted: November 21, 2006; DOI: 10.1002/macp.200600492

Keywords: photodecomposition; polycondensation; spin coating; structure–property relations; thin films

[1] [1a] T. Lippert, *Adv. Polym. Sci.* **2004**, *168,* 51; [1b] T. Lippert, T. Dickinson, *Chem. Rev.* **2003**, *103,* 453; [1c] T. Lippert, *Plasma Process. Polym.* **2005**, *2,* 525.
[2] [2a] S.-K. Chang-Jian, J.-R. Ho, J. J.-W. Cheng, C.-K. Sung, *Nanotechnology* **2006**, *17,* 1184; [2b] K. D. Kyrkis, A. A. Andreadaki, D. G. Papazoglou, I. Zergioti, "Direct Transfer

and Microprinting of Functional Materials by Laser-Induced Forward Transfer", in: *Recent Advances in Laser Processing of Materials*, J. Perrière, E. Millon, E. Fogarassy, Eds., Elsevier, Oxford 2006, Chapter 7, pp. 213–241; [2c] D. B. Chrisey, A. Pique, R. A. McGill, J. S. Horwitz, B. R. Ringeisen, D. M. Bubb, P. K. Wu, *Chem. Rev.* **2003**, *103,* 553.

[3] [3a] W. A. Tolbert, I.-Y. S. Lee, M. M. Doxtader, E. W. Ellis, D. D. Dlott, *J. Imaging Sci. Technol.* **1993**, *37,* 411; [3b] G. R. Pinto, *J. Imaging Sci. Technol.* **1994**, *38,* 565; [3c] M. Kinoshita, K. Hoshino, T. Kitamura, *J. Imaging Sci. Technol.* **2000**, *44,* 105.

[4] [4a] D. M. Karnakis, T. Lippert, N. Ichinose, S. Kawanishi, H. Fukumura, *Appl. Surf. Sci.* **1998**, *127–129,* 781; and references cited therein; [4b] H. Fukumura, *J. Photochem. Photobiol. A: Chem* **1997**, *106,* 3.

[5] [5a] B. Hopp, T. Smausz, N. Barna, C. Vass, Z. Antal, L. Kredics, *J. Phys. D: Appl. Phys.* **2005**, *38,* 833; [5b] J. M. Fernandez-Pradas, M. Colina, P. Serra, J. Dominguez, J. L. Morenza, *Thin Solid Films* **2004**, *453–454,* 27; [5c] J. A. Barron, P. Wu, H. D. Ladouceur, B. R. Ringeisen, *Biomed. Microdevices* **2004**, *6,* 139; [5d] B. R. Ringeisen, D. B. Chrisey, A. Pique, H. D. Young, R. Modi, M. Bucaro, J. Jones-Meehan, B. J. Spargo, *Biomaterials* **2002**, *23,* 161; [5e] I. Zergioti, A. Karaiskou, D. G. Papazoglou, C. Fotakis, M. Kapsetaki, D. Kafetzopoulos, *Appl. Surf. Sci.* **2005**, *247,* 584; [5f] A. S. Holmes, S. M. Saidam, *J. Microelectromech. Syst.* **1998**, *7,* 416; [5g] J. Y. Lee, S. T. Lee, *Adv. Mater.* **2004**, *16,* 51; [5h] M. C. Suh, B. D. Chin, M.-H. Kim, T. M. Kang, S. T. Lee, *Adv. Mater.* **2003**, *15,* 1254.

[6] M. B. Wolk, J. Baetzold, E. Bellmann, T. R. Hoffend, S. Lamansky, Y. Li, R. R. Roberts, V. Savvateev, J. S. Staral, W. A. Tolbert, *Proc. SPIE* **2004**, *5519,* 12.

[7] A. Doraiswamy, R. J. Narayan, T. Lippert, L. Urech, A. Wokaun, M. Nagel, B. Hopp, M. Dinescu, R. Modi, R. C. Y. Auyeung, D. B. Chrisey, *Appl. Surf. Sci* **2006**, *252,* 4743.

[8] O. Nuyken, J. Stebani, A. Wokaun, T. Lippert, "Polymers with Triazene Units in the Main Chain: Application for Laser-Lithography", in: *Macromolecular Engineering. Recent Advances*, M. K. Mishra, O. Nuyken, S. Kabayashi, Y. Yagci, B. Sar, Eds., Plenum Press, New York 1995, Chapter 23, pp. 303–318.

[9] [9a] J. Stebani, O. Nuyken, T. Lippert, A. Wokaun, *Makromol. Chem. Rapid Commun.* **1993**, *14,* 365; [9b] O. Nuyken, J. Stebani, T. Lippert, A. Wokaun, A. Stasko, *Macromol. Chem. Phys.* **1995**, *196,* 739; [9c] O. Nuyken, J. Stebani, T. Lippert, A. Wokaun, A. Stasko, *Macromol. Chem. Phys.* **1995**, *196,* 751.

[10] O. Nuyken, C. Scherrer, A. Baindl, A. R. Brenner, U. Dahn, R. Gärnter, S. Kaiser-Röhrich, R. Kollefrath, P. Matusche, B. Voit, *Prog. Polym. Sci.* **1997**, *22,* 93.

[11] [11a] J. Kritzenberger, D. Franzke, T. Kunz, A. Lang, O. Nuyken, A. Wokaun, *Angew. Makromol. Chem.* **1998**, *254,* 17; [11b] O. Nuyken, A. Lang, *Angew. Makromol. Chem.*, **1995**, *230,* 129; [11c] O. Nuyken, U. Dahn, W. Ehrfeld, V. Hessel, K. Hesch, J. Landsiedel, J. Diebel, *Chem. Mater.* **1997**, *9,* 485.

[12] [12a] M. N. Nobis, O. Nuyken, *Macromol. Chem. Phys.* **2001**, *202,* 2769; [12b] M. N. Nobis, C. Scherer, O. Nuyken, *Macromolecules* **1998**, *31,* 4806.

[13] [13a] A. F. Thünemann, U. Schnöller, O. Nuyken, B. Voit, *Macromolecules* **2000**, *33,* 5665; [13b] H. van Aert, M. van Damme, O. Nuyken, U. Schnöller, K.-J. Eichhorn, K. Grundke, B. Voit, *Macromol. Mater. Eng.* **2001**, *286,* 488.

[14] [14a] O. Nuyken, U. Dahn, *J. Polym. Sci. A* **1997**, *35,* 3017; [14b] Ch. Hahn, Th. Kunz, U. Dahn, O. Nuyken, A. Wokaun, *Appl. Surf. Sci.* **1998**, *1,* 899; [14c] N. Hoogen, O. Nuyken, *J. Polym. Sci. A* **2000**, *38,* 1903; [14d] J. Wei, N. Hoogen, T. Lippert, O. Nuyken, A. Wokaun, *J. Phys. Chem. B* **2001**, *105,* 1267; [14e] M. Eigner, H. Komber, B. Voit, *Macromol. Chem. Phys.* **2001**, *202,* 245.

[15] [15a] E. C. Buruiana, V. Niculescu, T. Buruiana, *J. Appl. Polym. Sci.* **2003**, *88,* 1203; [15b] E. C. Buruiana, V. Melinte, T. Buruiana, T. Lippert, H. Yoshikawa, H. Mashuhara, *J. Photochem. Photobiol. A* **2005**, *171,* 261[15c] E. C. Buruiana, T. Buruiana, H. Lenuta, T. Lippert, L. Urech, A. Wokaun, *J. Polym. Sci. A* **2006**, *44, published online.*

[16] T. Mito, T. Tsujita, H. Masuhara, N. Hayashi, K. Suzuki, *Jpn. J. Appl. Phys.* **2001**, *40,* L805.

[17] [17a] P. Griess, *Justus Liebigs Ann. Chem.* **1862**, *121,* 258; [17b] D. B. Kimball, M. M. Haley, *Angew. Chem. Int. Ed.* **2002**, *41,* 3338.

[18] T. B. Patrick, R. P. Willaredt, D. J. DeGonia, *J. Org. Chem.* **1985**, *50,* 2232.

[19] [19a] J. R. Beadle, S. H. Korzeniowski, D. E. Rosenberg, B. J. Garcia-Slange, G. W. Gokel, *J. Org. Chem.* **1984**, *49,* 1594; [19b] M. Gomberg, W. E. Bachmann, *J. Am. Chem. Soc.* **1924**, *46,* 2339; [19c] J. J. Li, "*Name Reactions: A Collection of Detailed Reaction Mechanisms.*" Springer Verlag, Berlin, Heidelberg, New York 2002, p. 143; and references cited therein; [19d] C. Rüchardt, E. Merz, *Tetrahedron Lett.* **1964**, *5,* 2431.

[20] [20a] D. S. Brown, M. P. Merrin, K. Vaughan, *Proc. N. S. Inst. Sci.* **1995**, *40,* 67; [20b] H. Jian, J. M. Tour, *J. Org. Chem.* **2005**, *70,* 3396; [20c] M. H. Akhtar, R. S. McDaniel, M. Feser, A. C. Oehlschlager, *Tetrahedron* **1968**, *24,* 3899; [20d] Th. Lippert, A. Wokaun, J. Dauth, O. Nuyken, *Magn. Res. Chem.* **1992**, *30,* 1178.

[21] J.-C. Panitz, T. Lippert, J. Stebani, O. Nuyken, A. Wokaun, *J. Phys. Chem.* **1993**, *97,* 5246.

[22] D. Enders, C. Rijksen, E. Bremus-Köbberling, A. Gillner, J. Köbberling, *Tetrahedron Lett.* **2004**, *45,* 2839.

[23] D. Franzke, J. Kritzenberger, E. E. Ortelli, A. Baindl, O. Nuyken, A. Wokaun, *J. Photochem. Photobiol. A* **1998**, *112,* 63.

[24] [24a] B. Eliasson, U. Kogelschatz, *Appl. Phys. B* **1988**, *46,* 299; [24b] U. Kogelschatz, *Pure Appl. Chem.* **1990**, *62,* 1667.

[25] J. Xu, J. Liu, D. Cui, M. Gerhold, A. Y. Wang, M. Nagel, T. K. Lippert, *Nanotechnology* **2007**, *18, published online 15 Dec 2006.*

Macromolecular Journals

DOI: 10.1002/macp.200600492